Chalcogenide Letters Vol. 20, No. 5, May 2023, p. 367 - 376

Structural, morphology and optical properties studies of Ni doped CdSe thin films

A. J. Jarjees Alsoofy[a], R. S. Ali[b*], Z. S. A. Mosa[c], N. F. Habubi[d], S.S. Chiad[e]
[a]*Department of Physics, College of Sciences, University of Mosul, Mosul, Iraq.*
[b]*Department of Physics, College of Science, Mustansiriyah University, Baghdad, Iraq.*
[c]*Department of Pharmacy, Al-Manara College for Medical Science, Iraq.*
[d]*Department of Radiation and Sonar Technologies, Alnukhba, University College, Baghdad, Iraq.*
[e]*Department of Physics, College of Education, Mustansiriyah University, Baghdad, Iraq.*

Thermal evaporation was used to prepare nickel (Ni) doped cadmium selenide thin films in different proportions (0, 1 and 3) wt.% on glass substrates at room temperature. According to XRD examination, all films possessed a polycrystalline hexagonal structure, with the (002) plane as the ideal orientation. According to AFM analysis, the average particle size decreases as the amount of doping increases, showing that the distribution of grains has become more uniform. The transmission and distortion ratios of the films were measured to learn more about their optical properties, which revealed that the (CdSe) films' transmittance decreased as the Ni films were doped, respectively. Additionally, it was discovered that all produced films had absorption coefficients larger than ($\alpha > 10^4\ cm^{-1}$) and that the value of this coefficient rises with increasing doping. The films exhibited all direct optical energy gaps, according to the findings (CdSe). As the doping fraction decreased, the gap values decreased from 1.72 eV to 1.62 eV.

(Received March 30, 2023; Accepted May 17, 2023)

Keywords: CdSe, Ni, Thin films, Thermal evaporation, XRD, AFM, Optical properties, Energy gap.

1. Introduction

CdSe has a direct band gap and good optical properties among the semiconductors. CdSe is commonly using in photovoltaic material with a high absorption coefficient and a band gap energy of 1.65 eV to 1.84 eV [1,2]. CdSe exists in hexagonal, cubic, and cubic rock salt crystal forms [3]. After annealing, it can be converted into a hexagonal wurtzite structure [4]. Because electrons are the primary charge carriers in CdSe, it is as an n-type negative electrical conductor [5]. CdSe is suited for photonic crystal manufacturing because of its high refractive index and low absorption [6]. CdSe thin films were fabricated using various deposition techniques, including CBD [7], spray pyrolysis [8], PLD [9], electrodeposition [10] and thermal evaporation [11, 12]. Many authors used dopant impurities to improve the performance of CdSe nanocrystalline thin films and created thin films of CdSe:Fe [13], CdSe:Co [14], CdSe:Cu [15] and CdSe:Mn [16-18], In this study, pure Cadmium Selenide films were grown by thermal evaporation along with Nb nanoparticles doped at different ratios.

2. Experimental

Ni-doped CdSe thin film samples were made using vacuum coating equipment and a thermal co-evaporation process in a vacuum of 2×10^{-5} torr. It is necessary to weigh a precise

* Corresponding author: reemphy81@uomustansiriyah.edu.iq
https://doi.org/10.15251/CL.2023.205.367

amount of Cadmium Selenide powder and place it in a molybdenum boat, take 1% and 3% of this weight in Ni and place it in a different molybdenum boat. Glass slides were employed as bases, and positioned directly above (CdSe and Ni) was used as source material at a distance of roughly 18 cm. The interference method was employed to measure film thickness in the range of (1μm), and the deposition rate was 50nm/min. An X-ray diffractometer was used to analyze the structural features of the produced thin films. Film surface was studied using an AFM. Employing a double beam spectrophotometer to estimate optical transmittance.

3. Results and discussions

3.1. XRD analysis

The hexagonal and cubic phases of CdSe: Ni exist. The XRD spectrum of Ni doped CdSe samples coated on glass is shown in Figure 1. The JCPDS card No (00-019-019) information for CdSe and Ni selenide was used to determine the sample phase. The XRD pattern suggests a polycrystalline structure. The study of spectrum indicates that all the film samples have hexagonal phase, all the films demonstrate three dominant peaks at 25.40°, 42.54° and 55.93° belonging to (002), (110) and (202) planes, respectively. As the doping samples are increased to (0.1 and 0.3) % the CdSe peaks increased slightly, respectively. The peak intensities attributed to CdSe crystallinity improved, and there was a relationship between crystallinity and FWHM values. While larger crystal sizes indicate an increase in film crystallinity, higher values of FWHM indicate a reduction in crystallinity [19]. The FWHM from undoped 0.94° and when doped in 3% Ni decreased to 0.86°.

Crystallite size (D) was calculated using Debye-Scherrer formula [20-23]:

$$D = \frac{k\lambda}{\beta cos\theta} \tag{1}$$

Where λ = 1.518 Å (CuK a radiation wavelength), θ is the Bragg's angle. D of CdSe thin films was determined to be 8.57nm, while for CdSe:Ni thin films it was determined to be 9.48nm. D ranged between (8.57 - 9.84) nm. A maximum crystallite size was obtained for the films deposited at 3% doping in Ni. Larger crystallites brought on a narrower FWHM and a strong interface between film and base. A device's outcomes are enhanced by good crystallization, confirmed by a large grain size, proving that CdSe is an excellent option for window layer. [24].

The following equation was used to calculate microstrain (ε) [25-27]:

$$\varepsilon = \frac{\beta cos\theta}{4} \tag{2}$$

The following equation was used to calculate dislocation density (δ) [28-30]:

$$\delta = \frac{1}{D^2} \tag{3}$$

If ε value is lower, the property is noncrystalline. A higher ε on the other hand, denotes a polycrystalline film. Lower values will result in fewer imperfections and higher crystallinity levels in films. It is observed from Figure 2 δ is found to decrease while increasing Ni concentrations from 1% and 3%. Studies on the functional dependence of ε, δ, and Ni doping show that the strain, dislocation density, and crystallite size decrease when Ni doping increases. There is a possibility that the expansion of the crystal lattice is caused by the larger radius of the dopant atoms [31]. Table 1 shows the structure parameter of all films.

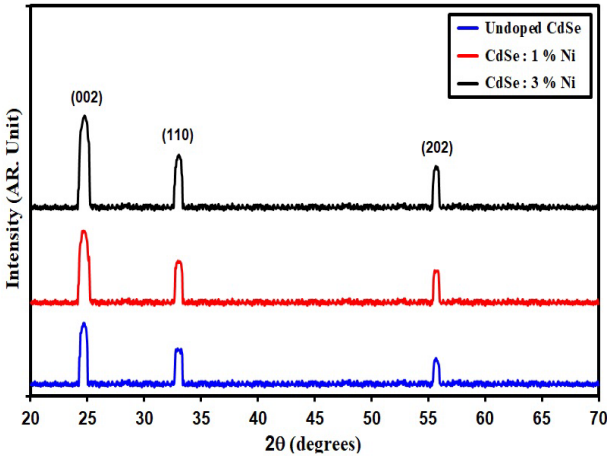

Fig. 1. XRD patterns of intended films.

Table 1. Structure parameter of intended films.

Specimen	2 θ (°)	(hkl) Plane	FWHM (°)	Optical bandgap (eV)	crystallite size (nm)	Dislocations density ($\times 10^{14}$) (lines/m^2)	Strain ($\times 10^{-4}$)
Undoped CdSe	25.40	002	0.94	1.72	8.57	136.56	40.43
CdSe: 1% Ni	25.36	002	0.90	1.67	9.05	122.90	38.30
CdSe: 3% Ni	25.31	002	0.86	1.62	9.48	111.27	36.61

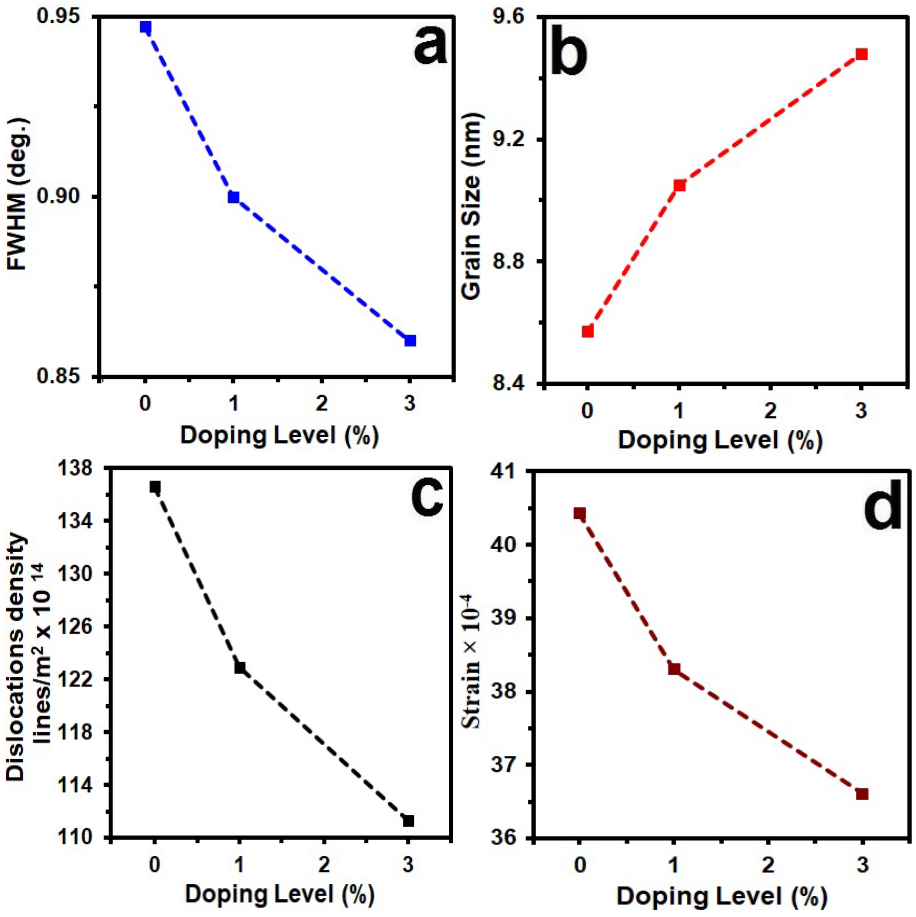

Fig. 2. X-ray parameter of intended CdSe films.

3.2. Surface topography study

Fig 3 shows the surface topography for the CdSe and CdSe:Ni by using AFM. The size of CdSe nanocrystals depends on the doping between CdSe and Ni.

As CdSe film surface has homogeneous features and grains of uniform size, as shown in the 3D image. Surface roughness is commonly measured using RMS roughness, this is defined as the surface height profile's standard deviation from the average [32]. RMS is approximately (7.82 nm to 4.2 nm). As doping levels increased, the average particle size decreased, indicating that grain dispersion became more uniform. The histograms of the growth of granular groups are shown in Figure 3. Table 2 shows that the root mean square of surface roughness reduced when doping levels grew. The image in Fig. 3 indicates the films nanostructure. The surface was clearly smooth, and the decrease in RMS of CdSe thin film resulted in greater crystalline development in the vertical direction than in the horizontal direction. Also visible was the rise in grain size due to increased doping, which resulted in surface homogeneity, consistent with XRD results [33].

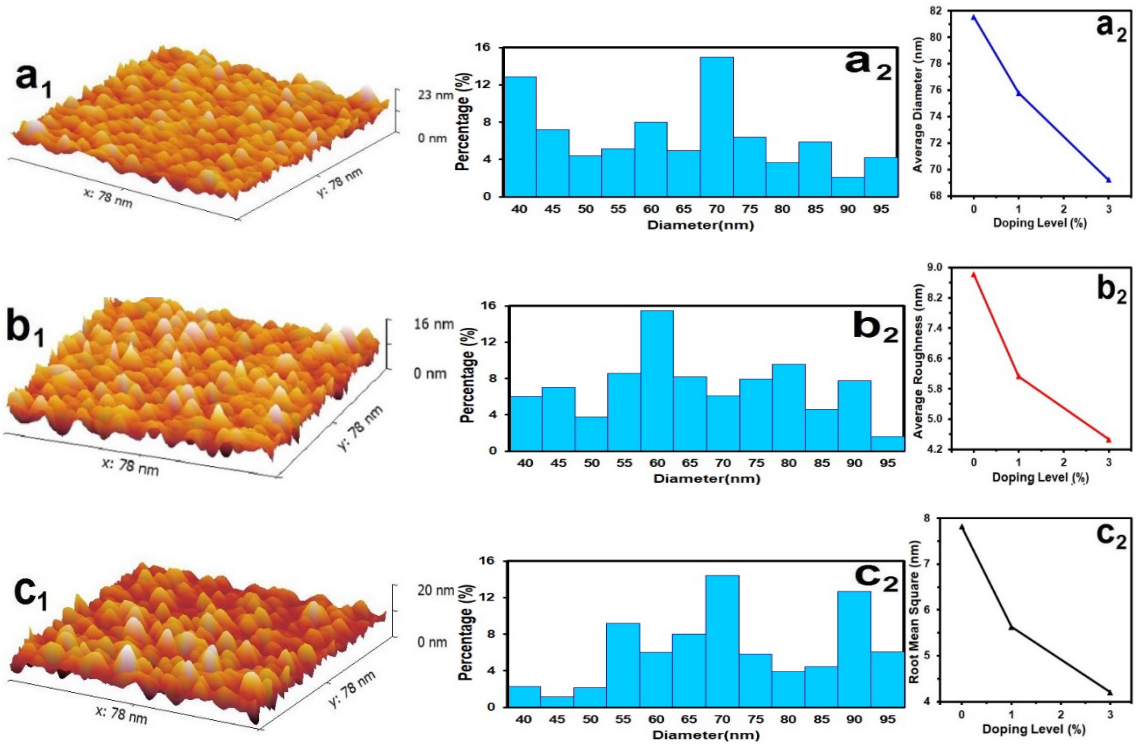

Fig. 3. AFM of grown films.

Table 2. AFM parameter of grown films.

Samples	Average Particle size nm	R_a (nm)	R. M. S. (nm)
Undoped CdSe	81.53	8.82	7.82
CdSe: 1% Ni	75.79	6.13	5.63
CdSe: 3% Ni	69.21	4.46	4.20

3.3. Optical properties study

For all produced films, transmittance spectrometry measurements were done in the wavelength region of 300-900 nm. Figure (4) demonstrates how the transmittance (T) spectrum of CdSe and CdSe changes as a function of wavelength: Ni films with various doping levels. Due to the incident waves being photons of varied energy, the transmittance behaviour for all films increases at short wavelengths (high photon energies), as seen in the figure. The figure

demonstrates that as the doping of the produced film is increased, the transmittance of the film decreases in general, Photons falling onto the film's surface will be successively absorbed by crystals within a single grain due to the film's crystallization level, restricting their capacity to be reflected or permeabilized without being absorbed by the electrons. The number of crystals in the film grows as the thickness of the film increases, resulting in total absorption and an increase in the absorption coefficient [34]. Figure (4) illustrates the transmittance (T) spectrum of Ni-doped CdSe films made by PVD as a function of wavelength (1 and 3 percent). As demonstrated in the figure, Wave transmittance of the faulty material has decreased with wavelength because of the density of local levels created by impurity atoms between the conduction and valence bands. The prepared pure cadmium selenide films recorded the greatest transmittance. As the doping concentration increases, the transmission diminishes, implying that Ni dopants have been absorbed into the trap levels of band gap [35].

The absorption coefficient α, is analyzed using the following relationship to find more. [36-38]:

$$\alpha = \frac{1}{d} ln \frac{1}{T} \tag{4}$$

Where d. is film thickness. Figure 5 depicts the variance of α . When doping concentration rises, the absorption coefficient rises as well. This reveals that scattered Ni dopants operate as trap centers. In CdSe thin films, Ni behaves as an n-type dopant. [39], With Ni-doping, for these additional electrons can boost α by incorporating the energy of incident photons into the absorption process via electron-photon interaction. All of the samples had a high visible absorption, making them a good choice for use as an absorber layer [40].

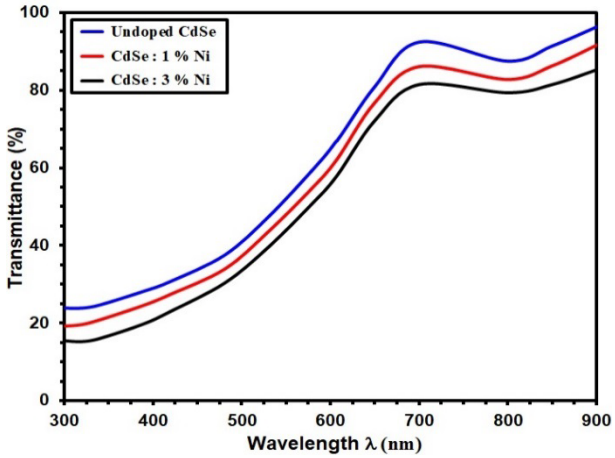

Fig. 4. T of grown films

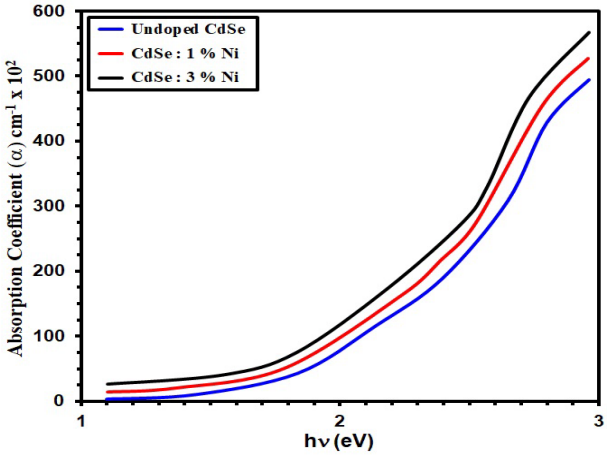

Fig. 5. α of the intended films.

Using the equation below, the optical energy band gap (e_g) was calculated by: [41-42]:

$$\alpha h\upsilon = B(h\upsilon - E_g)^{\frac{1}{2}} \quad (5)$$

B is a constant, B denotes a constant. Figure 6 illustrates the variation of $(\alpha h\upsilon)^2$ as a function of hυ. With increasing doping concentration, ni-doping reduces the optical energy band gap from 1.72 eV to 1.62 eV [43]. The shrinking of E_g relates to the extension of localized states in E_g as the band gap's tailing trap levels increase, reducing the area's breadth [44]. It could also be due to the introduction of dopant atoms into the host crystal structure, which increases lattice disorder [45]. Because E_g has shrunk, Ni-doping has the potential to improve optical absorption.

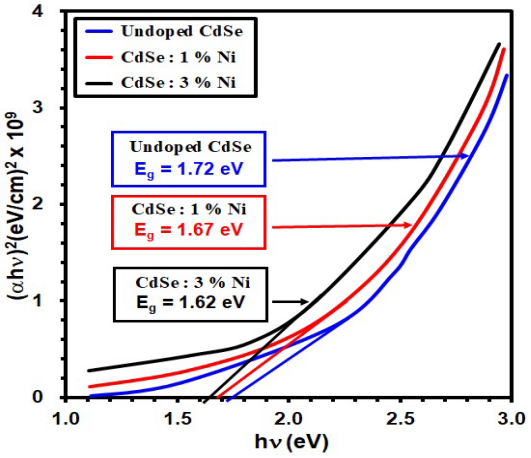

Fig. 6. (E_g) of intended films.

The extinction coefficient (*k*)was also calculated from Eqs. (6) [46-48]:

$$K = \frac{\alpha\lambda}{4\pi} \quad (6)$$

sing the relation, the refractive index (n) is estimated from the reflectance (R) data [49]:

$$R = \frac{(n-1)^2}{(n+1)^2} \quad (7)$$

The behavior of k of CdSe and (1and 3) % doped with Ni films are shown in Figure (7), As can be seen in this graph, the value of (k) rises as Ni doping increases. Figure (8) shows that the refractive index (n) is increased by increasing the concentration of Ni ions. The results of K and n show similar behavior, which could be related to the quantum size effect, crystallization improvement, and variations in the film's stoichiometry [50].

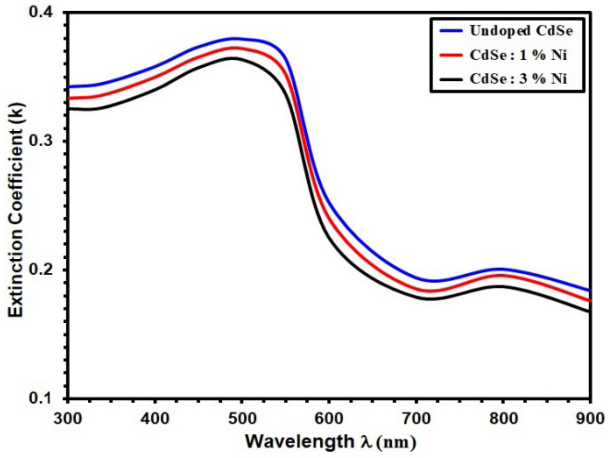

Fig. 7. k of grown films.

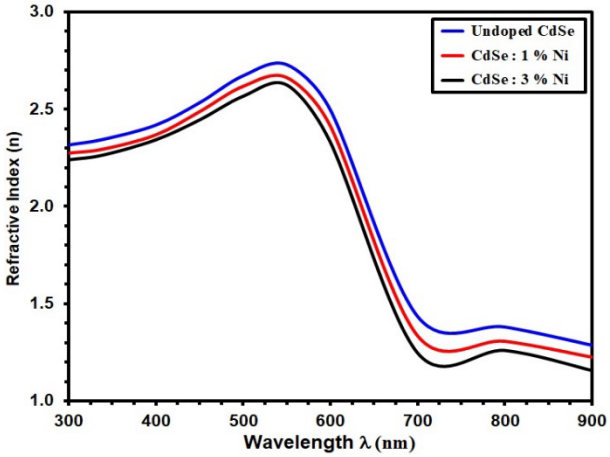

Fig. 8. n of grown films.

4. Conclusion

Doped CdSe and Ni PVD thin films of CdSe were successfully deposited in Ni utilizing varying doping levels. The films generated to have a hexagonal phase with a preference for orientation in the (002) plane., and they are nanocrystalline in nature, according to XRD investigations. AFM analysis revealed that the average particle size decreases with increasing doping, indicating that the distribution of grains became more uniform with the increasing doping. The thin materials' energy bandgap values range from 1.72 eV to 1.62 eV depending on Ni doping, with the pure CdSe serving as a control recording the greatest energy bandgap value of 1.72 eV.

Acknowledgments

Authors would thank Mustansiriyah University and Alnukhba University College for assisting them with their preventative efforts.

References

[1] T. C. Santhosh., K. V. Bangera, G. K. Shivakumar, Mater. Sci. Semicond. Process. 68, 114 (2017); https://doi.org/10..1016/j.mssp.2017.06.004

[2] R. Sahebi, M. R. Roknabadi, M. Behdani, Mater. Res. Express 6, 126453 (2019); https://doi.org/10.1088/2053-1591/ab6c17

[3] K. Sharma, A. S. Al-Kabbi, G. S. Saini, S. K. Tripathi, Materials Research Bulletin 47, 1400 (2012); https://doi.org/10.1016/j.materresbull.2012.03.008

[4] M. S. Kang, A. Sahu, D. J. Norris, C. D. Frisbie, Nano Lett. 10, 3727 (2010); https://doi.org/10.1021/nl102356x

[5] S. K. Tripathi, J. Mater. Sci. 45, 5468 (2010); https://doi.org/10.1007/s10853-010-4601-6

[6] E. El-Menyawy, A. A. Azab, Optik, 168, 217 (2018); https://doi.org/10.1016/j.ijleo.2018.04.056

[7] P. P. Hankare, V. M. Bhuse, K. M. Garadkar, S. D. Delekar, I. S. Mulla, Semicond. Sci. Technol. 19, 70 (2004); https://doi.org/10.1088/0268-1242/19/1/012

[8] A. A. Yadav, M. A. Barote, E. U. Masumdar, Mater. Chem. Phys. 121, 53 (2010); https://doi.org/10.1016/j.matchemphys.2009.12.039

[9] S. Thanikaikarasan, T. Mahalingam, M. Raja, Taekyu Kim, Yong Deak Kim, J. Mater. Sci. Mater. Electron 20, 727 (2009); https://doi.org/10.1007/s10854-008-9794-y

[10] K. Sharma, A. S. Al-Kabbi, G. S. Saini , S. K. Tripathi, Materials Research Bulletin 47, 1400 (2012); https://doi.org/10.1016/j.materresbull.2012.03.008

[11] E. S. Hassan, A. K. Elttayef, S. H. Mostafa, M. H. Salim, S. S. Chiad, Journal of Materials Science: Materials in Electronics, 30 (17), 15943-15951, (2019); https://doi.1007/s10854-019-01954-1

[12] Jasim, R.I., Hadi, E.H., Chiad, S.S., N. F. Habubi, Jadan, M., Addasi, J.S., Journal of Ovonic Research, 19(2), 187–196 (2023); https://doi.org/10.15251/JOR.2023.192.187

[13] D. Dangi and R. Dhar, Journal of integrated Science and technology. Vol 4, No 1(2016); https://doi.10.1007/s10854-014-1918-y

[14] J. Singh, N.K. Verma, Journal of Superconductivity and Novel Magnetism, 27, 2371-2377 (2014); https://doi.10.1007/s10948-014-2603-3.

[15] J. Sivasankar, P. Mallikarjana, M. Rigana Begam, N. Madhusudhana Rao, S. Kaleemulla, J. Subrahmanyam, Journal of Materials Science: Materials in Electronics, 27, 2300-2304 (2016); https://doi.10.1007/s10854-015-4025-9

[16] T. Shen, J. Tian, L. Lv, C. Fei, Y. Wang, T. Pulleritsc, G. Cao, Electrochimica Acta, 191, 62-69 (2016); https://doi.org/10.1016/j.electacta.2016.01.056

[17] J. Singh, S. Kumar, N.K. Verma, Materials Science in Semiconductor Processing, 26, 1-6 (2014); https://doi.org/10.1016/j.mssp.2014.03.032.

[18] S. B. Singh, M.V. Limaye, S. K . Date, S. Gokhale and S. K. Kulkarni, Physics review B, 80, 235421(2009); https://doi.org/10.14445/23500301/IJAP-V8I2P106

[19] B. Singh, J. Singh, R. Kaur, R. K. Moudgil, S. K. Tripathi, RSC Adv. 7, 53951 (2017); https://doi.org/10.1039/C7RA02904G

[20] E. H. Hadi, D. A. Sabur, S. S. Chiad, N. F. Habubi, K. H. Abass, Journal of Green Engineering, 10 (10), 8390 (2020); https://doi.org/10.1063/5.0095169

[21] H. A. Hussin, R. S. Al-Hasnawy, R. I. Jasim, N. F. Habubi, S. S. Chiad, Journal of Green Engineering, 10(9), 7018 (2020); https://doi.org/10.1088/1742-6596/1999/1/012063

[22] D. M. A. Latif, S. S. Chiad, M. S. Erhayief, K. H. Abass, N. F. Habubi, H. A. Hussin, Journal of Physics, Conference Series 1003(1), 012108 (2018); https://doi.org/10.1088/1742-6596/1003/1/012108

[23] A. L. Efros, M. R. Annu, Rev. Mater. Sci. 30, 475 (2000); https://doi.org/10.1146/annurev.matsci.30.1.475

[20] M. D. Sakhil, Z. M. Shaban, K. S. Sharba, N. F. Habub, K. H. Abass, S. S. Chiad, A. S. Alkelaby, NeuroQuantology, 18 (5), 56 (2020); https://doi.org/10.14704/nq.2020.18.5.NQ20168

[21] A. J. Ghazai, O. M. Abdulmunem, K. Y. Qader, S. S. Chiad, N. F. Habubi, AIP Conference Proceedings 2213 (1), 020101 (2020); https://doi.org/10.1063/5.0000158

[22] M. R. Bhuiyan, M. A. Azad, S. M. Hasan, Indian Journal of pure and Applied Physics, 49, 180 (2011); https://doi.org/10.1016/j.clema.2021.100030

[23] M. S. Othman, K. A. Mishjil, H. G. Rashid, S. S. Chiad, N. F. Habubi, I. A. Al-Baidhany, Journal of Materials Science: Materials in Electronics, 31(11), 9037 (2020); https://doi.org/10.1007/s10854-020-03437-0

[24] R. S. Ali, H. S. Rasheed, N. F. Habubi, S. S. Chiad, Letters, 20(1), 63 (2023); https://doi.org/10.15251/CL.2023.201.6

[25] H. T. Salloom, E. H. Hadi, N. F. Habubi, S. S. Chiad, M. Jadan, J. S. Addasi, Digest Journal of Nanomaterials and Biostructures, 15 (4), 189 (2020); https://doi.org/10.15251/DJNB.2020.154.1189

[26] S. S. Chiad, H. A. Noor, O. M. Abdulmunem, N. F. Habubi, M. Jadan, J. S. Addasi, Journal of Ovonic Research, 16 (1), 35 (2020).

[27] R. S. Ali, M. K. Mohammed, A. A. Khadayeir, Z. M. Abood, N. F. Habubi and S. S. Chiad, Journal of Physics: Conference Series, 1664 (1), 012016 (2020); https://doi:10.1088/1742-6596/1664/1/012016

[28] N. N. Jandow, M. S. Othman, N. F. Habubi, S. S. Chiad, K. A. Mishjil, I. A. Al-Baidhany, Materials Research Express, 6 (11), 116434 (2020); https://doi.org/10.1088/2053-1591/ab4af8

[29] E. S. Hassan, A. K. Elttayef, S. H. Mostafa, M. H. Salim and S. S. Chiad. Journal of aterials Science: Materials in Electronics, 30 (17),15943 (2019); https://doi.org/10.1155/2014/684317

[30] R. Sahebi, M. R. Roknabadi, M. Behdani, Optik 204, 164204 (2020); https://doi.org/10.1016/j.ijleo.2020.164204

[31] K. Girija, S. Thirumalairajan, S. M. Mohan, J. Chandrasekaran, Chalocogenide Letters 6(8), 351 (2009); https://doi.org/10.15251/CL.2022.1912.901

[32] N. Y. Jamil, M. T. Mahmood, N. A. Mustafa, Rafidain Journal of Science, 23 (1) 116 (2012); https://doi.org/10.33899/rjs.2012.29447

[33] S. Mathuri, K. Ramamurthi, R. R. Babu, Thin Solid Film 625, 138 (2017); https://doi.org/10.1016/j.tsf.2017.01.053

[34] Y. M. Niquet, G. Allan, C. Deleue, M. Lannoo, Appl. Phys. Lett. 77, 1182 (2000); https://doi.org/10.1063/1.1289659

[35] S. S. Chiad, A. S. Alkelaby, K. S. Sharba, Journal of Global Pharma Technology, 11(7), 662 (2020); https://doi:10.14704/nq.2020.18.5.NQ20168

[36] N. Y. Ahmed, B. A. Bader, M. Y. Slewa, N. F. Habubi, S. S. Chiad, NeuroQuantology, 18(6), 55 (2020); https://doi.org/10.14704/nq.2020.18.6.NQ20183

[37] A. A. Khadayeir, R. I. Jasim, S. H. Jumaah, N. F, Habubi, S. S. Chiad, Journal of Physics: Conference Series,1664, 012009 (2020); https://doi.org/10.1088/1742-6596/1664/1/012009

[38] Y. Azizian-Kalandaragh, A. Khodayari, Materials Science in Semiconductor Processing, 13 (2010) 225-230, 10.1016/j.mssp.2010.10.018.

[39] M.P. Deshpande, N. Garg, S.V. Bhatt, P. Sakariya, S.H. Chaki, Materials Science in Semiconductor Processing, 16 (2013) 915-922, DOI: 10.1016/j.mssp.2013.01.019.

[40] E. S. Hassan, K. Y. Qader, E. H. Hadi, S. S. Chiad, N. F. Habubi, K. H. Abass, Nano Biomedicine and Engineering, 12(3), 205 (2020); https://doi.org/10.5101/nbe.v12i3.p205-213

[41] R. S. Ali, N. A. H. Al Aaraji, E. H. Hadi, N. F. Habubi, S. S. Chiad, Journal of Nanostructuresthis link is disabled, 10(4), 810 (2020); https://doi: 10.22052/jns.2020.04.014

[42] Ali, R.S., Rasheed, H.S., Habubi, N.F., Chiad, S.S, Chalcogenide Lettersthis, 20 (1), 63–72 (2023); https://doi.org/10.15251/CL.2023.201.63

[43] H. T. Tung, D. V. Thuan, J. H. Kiat, D. H. Phuc, Appl. Phys. A 125, 505 (2019); https://doi.org/10.1007/s00339-019-2797-0

[44] K. Punitha, R. Sivakumar, C. Sanjeeviraja, V. Sathe, V. Ganesan, Appl. Surf. Sci. 344, 89 (2015); https://doi.org/10.1016/j.apsusc.2015.03.095

[45] F. Haque, K. S. Rahman, Akhtaruzzaman, H. Abdullah, T. S. Kiong, N. Amin, S. K. Tiong, Mater. Res. Express 5, 096409 (2018); https://doi.org/10.1088/2053-1591/aad6c6

[46] S. S. Chiad, H. A. Noor, O. M. Abdulmunem, N. F. Habubi, M. Jadan, J. S. Addasi, Journal of Ovonic Research, 16 (1), 35-40 (2020).

[47] Sulaiman, H.T., Ali, R.S., Khoudhair, M.J., Mohammed, S.A.A., NeuroQuantologythis, 18(1), 99–102 (2020); https://doi.org/10.14704/nq.2020.18.1.NQ20113

[48] Sahoo, S.K., Mangal, S., Mishra, D., Kumar, P., Singh, U.P., Mater. Sci. Semicond. Process., 63, 76–82 (2017); https://doi.org/10.1016/j.mssp.2017.05.029

[49] N. Y. Ahmed, B. A. Bader, M. Y. Slewa, N. F. Habubi, S. S. Chiad, NeuroQuantology, 18(6), 55-60 (2020); https://doi.org/10.14704/nq.2020.18.6.NQ20183

[50] K. Punitha, R. Sivakumar, C. Sanjeeviraja, V. Sathe, V. Ganesan, J. Appl. Phys. 116, 213502 (2014); https://doi.org/10.1063/1.4903320